

Second Topological Moment $\langle m^2 \rangle$ of Two Closed Entangled Polymers

Franco Ferrari⁽¹⁾ Hagen Kleinert⁽²⁾ and Ignazio Lazzizzera⁽¹⁾

⁽¹⁾*Dipartimento di Fisica, Università di Trento, I-38050 Povo, Italy
and INFN, Gruppo Collegato di Trento.*

⁽²⁾*Institut für Theoretische Physik,
Freie Universität Berlin, Arnimallee 14, D-14195 Berlin, Germany.
(February 2000)*

We calculate exactly by field theoretical techniques the second topological moment $\langle m^2 \rangle$ of entanglement of two closed polymers P_1 and P_2 . This result is used to estimate approximately the mean square average of the linking number of a polymer P_1 in solution with other polymers.

1. Consider two closed polymers P_1 and P_2 which statistically can be linked with each other any number of times $m = 0, 1, 2, \dots$. The situation is illustrated in Fig. 1 for $m = 2$.

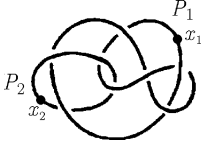


FIG. 1. Closed polymers P_1, P_2 with trajectories C_1, C_2 respectively.

An important physical quantity is the probability distribution of the linking number m as a function of the lengths of P_1 and P_2 . As a first step towards finding it we calculate, in this note, an exact expression for the second moment of the distribution, $\langle m^2 \rangle$.

An approximate result for this quantity was obtained before in Ref. [1] on the basis of a mean-field method, considering the density of bond vectors of P_2 as Gaussian random variables. Such methods are usually quite accurate when a large number of polymers is involved [2,3]. As an unpleasant feature, however, they introduce a dependence on the source of Gaussian noise, and modify the critical behavior of the system, whereas topological interactions are not expected to do that [4,5]. Our note goes therefore an important step beyond this approximation. It treats the two-polymer problem exactly, and contains an application to the topological entanglement in diluted solutions. The relevance of the two-polymer systems to such systems was emphasized in [1]. Focusing attention upon a particular molecule, P_1 , one may imagine all others to form a single long effective molecule P_2 .

2. Let $G_m(\mathbf{x}_1, \mathbf{x}_2; L_1, L_2)$ be the configurational probability to find the polymer P_1 of length L_1 with fixed coinciding end points at \mathbf{x}_1 and the polymer P_2 of length L_2 with fixed coinciding end points at \mathbf{x}_2 , topologically entangled with a Gaussian linking number m .

The second moment $\langle m^2 \rangle$ is defined by the ratio of integrals [6]

$$\langle m^2 \rangle = \frac{\int d^3x_1 d^3x_2 \int_{-\infty}^{+\infty} dm m^2 G_m(\mathbf{x}_1, \mathbf{x}_2; L_1, L_2)}{\int d^3x_1 d^3x_2 \int_{-\infty}^{+\infty} dm G_m(\mathbf{x}_1, \mathbf{x}_2; L_1, L_2)} \quad (1)$$

The denominator in (1) plays the role of a partition function:

$$Z \equiv \int d^3x_1 d^3x_2 \int_{-\infty}^{+\infty} dm G_m(\mathbf{x}_1, \mathbf{x}_2; L_1, L_2). \quad (2)$$

Due to the translational invariance of the system, the probabilities depend only on the differences between the end point coordinates:

$$G_m(\mathbf{x}_1, \mathbf{x}_2; L_1, L_2) = G_m(\mathbf{x}_1 - \mathbf{x}_2; L_1, L_2). \quad (3)$$

Thus, after a shift of variables, the spatial double integrals in (1) can be rewritten as

$$\int d^3x_1 d^3x_2 G_m(\mathbf{x}_1 - \mathbf{x}_2; L_1, L_2) = V \int d^3x G_m(\mathbf{x}; L_1, L_2),$$

where V denotes the total volume of the system.

3. The most efficient way of describing the statistical fluctuations of the polymers P_1 and P_2 is by two complex polymer fields $\psi_1^{a_1}(\mathbf{x}_1)$ and $\psi_2^{a_2}(\mathbf{x}_2)$ with n_1 and n_2 replicas ($a_1 = 1, \dots, n_1$, $a_2 = 1, \dots, n_2$). At the end we shall take $n_1, n_2 \rightarrow 0$ to ensure that these fields describe only one polymer each [7].

For these fields we define an auxiliary probability $G_\lambda(\vec{\mathbf{x}}_1, \vec{\mathbf{x}}_2; \vec{z})$ to find the polymer P_1 with open ends at $\mathbf{x}_1, \mathbf{x}'_1$ and the polymer P_2 with open ends at $\mathbf{x}_2, \mathbf{x}'_2$. The double vectors $\vec{\mathbf{x}}_1 \equiv (\mathbf{x}_1, \mathbf{x}'_1)$ and $\vec{\mathbf{x}}_2 \equiv (\mathbf{x}_2, \mathbf{x}'_2)$ collect initial and final endpoints of the two polymers P_1 and P_2 . Here we follow the approach of Edwards [8], in which one starts with open polymers with fixed ends. The case of closed polymers, where m becomes a true topological number and it is thus relevant in the present context, is recovered in the limit of coinciding extrema. We notice that in this way one introduces in the configurational probability an artificial dependence on the fixed points \mathbf{x}_1 and \mathbf{x}_2 . In physical situations, however, the fluctuations of the polymers are entirely free. For this reason we have averaged in (1) over all possible fixed points by means of the integrations in $d^3\mathbf{x}_1 d^3\mathbf{x}_2$.

The auxiliary probability $G_\lambda(\vec{\mathbf{x}}_1, \vec{\mathbf{x}}_2; \vec{z})$ is given by a functional integral [5]

$$G_\lambda(\vec{\mathbf{x}}_1, \vec{\mathbf{x}}_2; \vec{z}) = \lim_{n_1, n_2 \rightarrow 0} \int \mathcal{D}(\text{fields}) \times \psi_1^{a_1}(\mathbf{x}_1) \psi_1^{*a_1}(\mathbf{x}'_1) \psi_2^{a_2}(\mathbf{x}_2) \psi_2^{*a_2}(\mathbf{x}'_2) e^{-A}, \quad (4)$$

where $\mathcal{D}(\text{fields})$ indicates the measure of functional integration and a_1, a_2 are now fixed replica indices. $\mathcal{A} = \mathcal{A}_{\text{CS}} + \mathcal{A}_{\text{pol}}$ is the action governing the fluctuations. It consists of a polymer action

$$\mathcal{A}_{\text{pol}} = \sum_{i=1}^2 \int d^3 \mathbf{x} [|\bar{\mathbf{D}}^i \Psi_i|^2 + m_i^2 |\Psi_i|^2]. \quad (5)$$

and a Chern-Simons action to describe the linking number m

$$\mathcal{A}_{\text{CS}} = i\kappa \int d^3 x \varepsilon_{\mu\nu\rho} A_1^\mu \partial_\nu A_2^\rho, \quad (6)$$

In Eq. (6) we have omitted a gauge fixing term, which enforces the Lorentz gauge. The effects of self-entanglement and of the so-called *excluded-volume* interactions are ignored. The Chern-Simons fields are coupled to the polymer fields by the covariant derivatives $\mathbf{D}^i = \nabla + i\gamma_i \mathbf{A}^i$, with the coupling constants $\gamma_{1,2}$ given by $\gamma_1 = \kappa$, $\gamma_2 = \lambda$. The square masses of the polymer fields are given by $m_i^2 = 2Mz_i$, where $M = 3/a$, with a being the length of the polymer links, and z_i the chemical potentials of the polymers, measured in units of the temperature. The chemical potentials are conjugate variables to the length parameters L_1 and L_2 , respectively. The symbols Ψ_i collect the replicas $\psi_i^{a_i}$ of the two polymer fields. Let us note that in the topological Landau-Ginzburg model (4) the Chern-Simons fields do not change the critical behavior of the system, as expected.

The parameter λ is conjugate to the linking number m . We can therefore calculate the desired probability $G_m(\vec{\mathbf{x}}_1, \vec{\mathbf{x}}_2; L_1, L_2)$ from the auxiliary one $G_\lambda(\vec{\mathbf{x}}_1, \vec{\mathbf{x}}_2; \vec{z})$ by Laplace integrals over $\vec{z} = (z_1, z_2)$ and an inverse Fourier transformation over λ .

4. Let us use the polymer field theory to calculate the partition function (2). It is given by the integral over the auxiliary probabilities

$$Z = \int d^3 x_1 d^3 x_2 \lim_{\substack{\mathbf{x}'_1 \rightarrow \mathbf{x}_1 \\ \mathbf{x}'_2 \rightarrow \mathbf{x}_2}} \int_{c-i\infty}^{c+i\infty} \frac{Mdz_1}{2\pi i} \frac{Mdz_2}{2\pi i} e^{z_1 L_1 + z_2 L_2} \times \int_{-\infty}^{+\infty} dm \int_{-\infty}^{+\infty} d\lambda e^{-im\lambda} G_\lambda(\vec{\mathbf{x}}_1, \vec{\mathbf{x}}_2; \vec{z}). \quad (7)$$

The integration over m is trivial and gives $2\pi\delta(\lambda)$, enforcing $\lambda = 0$, so that

$$Z = \int d^3 x_1 d^3 x_2 \lim_{\substack{\mathbf{x}'_1 \rightarrow \mathbf{x}_1 \\ \mathbf{x}'_2 \rightarrow \mathbf{x}_2}} \int_{c-i\infty}^{c+i\infty} \frac{Mdz_1}{2\pi i} \frac{Mdz_2}{2\pi i} e^{z_1 L_1 + z_2 L_2} \times G_{\lambda=0}(\vec{\mathbf{x}}_1, \vec{\mathbf{x}}_2; \vec{z}). \quad (8)$$

To calculate $G_{\lambda=0}(\vec{\mathbf{x}}_1, \vec{\mathbf{x}}_2; \vec{z})$ we observe that the action \mathcal{A} is quadratic in λ . A trivial calculation gives

$$G_{\lambda=0}(\vec{\mathbf{x}}_1, \vec{\mathbf{x}}_2; \vec{z}) = \int \mathcal{D}(\text{fields}) e^{-\mathcal{A}_0} \times \psi_1^{a_1}(\mathbf{x}_1) \psi_1^{*a_1}(\mathbf{x}'_1) \psi_2^{a_2}(\mathbf{x}_2) \psi_2^{a_2}(\mathbf{x}') \quad (9)$$

where

$$\mathcal{A}_0 \equiv \mathcal{A}_{\text{CS}} + \int d^3 \mathbf{x} \left[|\mathbf{D}_1 \Psi_1|^2 + |\nabla \Psi_2|^2 + \sum_{i=1}^2 m_i^2 |\Psi_i|^2 \right], \quad (10)$$

From Eq. (10) it is clear that $G_{\lambda=0}(\vec{\mathbf{x}}_1, \vec{\mathbf{x}}_2; \vec{z})$ is the product of the configurational probabilities of two free polymers. In fact, the fields Ψ_2, Ψ_2^* are free, whereas the fields Ψ_1, Ψ_1^* are apparently not free because of the couplings with the Chern-Simons fields through the covariant derivative \mathbf{D}^1 . This is, however, an illusion: Integrating out A_2^μ in (9), we find the flatness condition: $\varepsilon^{\mu\nu\rho} \partial_\nu A_\mu^i = 0$. On a flat space with vanishing boundary conditions at infinity this implies $A_1^\mu = 0$. As a consequence, the functional integral (9) factorizes

$$G_{\lambda=0}(\vec{\mathbf{x}}_1, \vec{\mathbf{x}}_2; \vec{z}) = G_0(\mathbf{x}_1 - \mathbf{x}'_1; z_1) G_0(\mathbf{x}_2 - \mathbf{x}'_2; z_2), \quad (11)$$

where $G_0(\mathbf{x}_i - \mathbf{x}'_i; z_i)$ are the free correlation functions of the polymer fields

$$G_0(\mathbf{x}_i - \mathbf{x}'_i; L_i) = \int_{c-i\infty}^{c+i\infty} \frac{Mdz_i}{2\pi i} e^{z_i L_i} G_0(\mathbf{x}_i - \mathbf{x}'_i; z_i) = \frac{1}{2} \left(\frac{M}{4\pi L_i} \right)^{3/2} e^{-M(\mathbf{x}_i - \mathbf{x}'_i)^2 / 2L_i}. \quad (12)$$

Thus we obtain for (8) the integral

$$Z = 2\pi \int d^3 x_1 d^3 x_2 \lim_{\substack{\mathbf{x}'_1 \rightarrow \mathbf{x}_1 \\ \mathbf{x}'_2 \rightarrow \mathbf{x}_2}} G_0(\mathbf{x}_1 - \mathbf{x}'_1; L_1) G_0(\mathbf{x}_2 - \mathbf{x}'_2; L_2),$$

yielding the partition function

$$Z = \frac{2\pi M^3 V^2}{(4\pi)^3} (L_1 L_2)^{-3/2}. \quad (13)$$

It is important to realize that in Eq. (7) the limits of coinciding end points $\mathbf{x}'_i \rightarrow \mathbf{x}_i$ and the inverse Laplace transformations do not commute unless a proper renormalization scheme is chosen to eliminate the divergences caused by the insertion of the composite operators $|\psi_i^{a_i}(\mathbf{x})|^2$ and $|\Psi_i(\mathbf{x})|^2$.

5. Let us now turn to the numerator in Eq. (1). Exploiting the identity $m^2 e^{-im\lambda} = -\partial^2 e^{-im\lambda} / \partial \lambda^2$, and performing two partial integrations in λ , the same technique used above to evaluate the partition function Z yields

$$N = \kappa^2 \int d^3 x_1 d^3 x_2 \lim_{\substack{n_1 \rightarrow 0 \\ n_2 \rightarrow 0}} \int_{c-i\infty}^{c+i\infty} \frac{Mdz_1}{2\pi i} \frac{Mdz_2}{2\pi i} e^{z_1 L_1 + z_2 L_2} \times \int \mathcal{D}(\text{fields}) \exp(-\mathcal{A}_0) |\psi_1^{a_1}(\mathbf{x}_1)|^2 |\psi_2^{a_2}(\mathbf{x}_2)|^2 \times \left[\left(\int d^3 x \mathbf{A}_1 \cdot \Psi_1^* \nabla \Psi_1 \right)^2 + \frac{1}{2} \int d^3 x \mathbf{A}_1^2 |\Psi_1|^2 \right] \times \left[\left(\int d^3 x \mathbf{A}_2 \cdot \Psi_2^* \nabla \Psi_2 \right)^2 + \frac{1}{2} \int d^3 x \mathbf{A}_2^2 |\Psi_2|^2 \right]. \quad (14)$$

where \mathcal{A}_0 has been defined in (10). In the above equation we have taken the limits of coinciding endpoints inside the Laplace integral over z_1, z_2 . This will be justified later on the grounds that the potentially dangerous Feynman diagrams containing the insertions of operations like $|\Psi_i|^2$ vanish in the limit $n_1, n_2 \rightarrow 0$. The functional integral in Eq. (14) can be calculated exactly by diagrammatic methods since only four diagrams shown in Fig. (2) contribute.

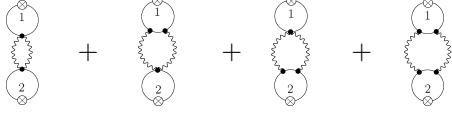


FIG. 2. Four diagrams contributing in Eq. (14). The lines indicate correlation functions of Ψ_i -fields. The crossed circles with label i denote the insertion of $|\psi_i^{a_i}(\mathbf{x}_i)|^2$.

Only the first diagram in Fig. 2 is divergent from the loop integral formed by two correlation functions of the vector field. This infinity may be absorbed in the four- Ψ interaction accounting for the excluded volume effect which we do not consider at the moment. No divergence arises from the insertion of the composite fields $|\psi_i^{a_i}(\mathbf{x}_i)|^2$.

6. In this section we evaluate the first term appearing in the right hand side of Eq. (14):

$$N_1 = \frac{\kappa^2}{4} \lim_{\substack{n_1 \rightarrow 0 \\ n_2 \rightarrow 0}} \int_{c-i\infty}^{c+i\infty} \frac{Mdz_1}{2\pi i} \frac{Mdz_2}{2\pi i} e^{z_1 L_1 + z_2 L_2} \int d^3 x_1 d^3 x_2 \int d^3 x'_1 d^3 x'_2 \left\langle |\psi_1^{a_1}(\mathbf{x}_1)|^2 |\psi_2^{a_2}(\mathbf{x}_2)|^2 (|\Psi_1|^2 \mathbf{A}_1^2)_{\mathbf{x}'_1} (|\Psi_2|^2 \mathbf{A}_2^2)_{\mathbf{x}'_2} \right\rangle. \quad (15)$$

There is an ultraviolet-divergence which must be regularized. This is done by cutting the spatial integrals off at the persistence length ξ over which a polymer is stiff. This contains the stiffness caused by the excluded-volume effects. To be rigorous, we define the integral (15) on a lattice with spacing ξ .

Replacing the expectation values by the Wick contractions corresponding to the first diagram in Fig. 2, we obtain

$$N_1 = \frac{V}{4\pi} \frac{M^4}{(4\pi)^6} (L_1 L_2)^{-\frac{1}{2}} \int_0^1 ds [(1-s)s]^{-\frac{3}{2}} \int d^3 x e^{-\frac{M\mathbf{x}^2}{2s(1-s)}} \times \int_0^1 dt [(1-t)t]^{-\frac{3}{2}} \int d^3 y e^{-\frac{M\mathbf{y}^2}{2t(1-t)}} \int d^3 x'_1 \frac{1}{|\mathbf{x}'_1|^4}.$$

The variables \mathbf{x} and \mathbf{y} have been rescaled with respect to the original ones in order to extract the behavior of N_1 in L_1 and L_2 . As a consequence, the lattices where \mathbf{x} and \mathbf{y} are defined have now spacings $\xi/\sqrt{L_1}$ and $\xi/\sqrt{L_2}$ respectively. The \mathbf{x}, \mathbf{y} integrals may be explicitly computed by analytical methods in the physical limit $L_1, L_2 \gg \xi$, in which the above spacings become small. This has a physical explanation. Indeed, if the polymer lengths are

much larger than the persistence length, the effects due to the finite monomer size become negligible and can be ignored.

Finally, it is possible to approximate the integral in \mathbf{x}'_1 with an integral over a continuous variable ρ and a cutoff in the ultraviolet region: $\int d^3 x'_1 1/|\mathbf{x}'_1|^4 \sim 4\pi^2 \int_{\xi}^{\infty} d\rho/\rho^2$. After these approximations, we obtain

$$N_1 = V \sqrt{\pi} \frac{M}{(4\pi)^3} (L_1 L_2)^{-1/2} \xi^{-1}. \quad (16)$$

7. For the second diagram in Fig. 2 we have to calculate

$$N_2 = \kappa^2 \lim_{\substack{n_1 \rightarrow 0 \\ n_2 \rightarrow 0}} \int_{c-i\infty}^{c+i\infty} \frac{Mdz_1}{2\pi i} \frac{Mdz_2}{2\pi i} e^{z_1 L_1 + z_2 L_2} \times \int d^3 x_1 d^3 x_2 \int d^3 x'_1 d^3 x'_2 \times \left\langle |\psi_1^{a_1}(\mathbf{x}_1)|^2 |\psi_2^{a_2}(\mathbf{x}_2)|^2 (\mathbf{A}_1 \cdot \Psi_1^* \nabla \Psi_1)_{\mathbf{x}'_1} \times (\mathbf{A}_1 \cdot \Psi_1^* \nabla \Psi_1)_{\mathbf{x}'_1'} (\mathbf{A}_2^2 |\Psi_2|^2)_{\mathbf{x}'_2} \right\rangle. \quad (17)$$

The above amplitude has no ultraviolet divergence, so that no regularization is required. The Wick contractions pictured in the second Feynman diagrams of Fig. 2 lead to the integral

$$N_2 = -4\sqrt{2} V L_2^{-1/2} L_1^{-1} \frac{M^3}{\pi^6} \int_0^1 dt \int_0^t dt' C(t, t'), \quad (18)$$

where $C(t, t')$ is a function independent of L_1 and L_2 :

$$C(t, t') = [(1-t)t'(t-t')]^{-3/2} \int d^3 x d^3 y d^3 z e^{-\frac{M(\mathbf{y}-\mathbf{x})^2}{2(1-t)}} \times \left(\nabla_{\mathbf{y}}^\nu e^{-M\mathbf{y}^2/2t'} \right) \left(\nabla_{\mathbf{x}}^\mu e^{-M\mathbf{x}^2/2(t-t')} \right) P_{\mu\nu}(\mathbf{x}, \mathbf{y}, \mathbf{x}),$$

with

$P_{\mu\nu}(\mathbf{x}, \mathbf{y}, \mathbf{x}) \equiv [\delta_{\mu\nu} \mathbf{z} \cdot (\mathbf{z} + \mathbf{x}) - (z+x)_\mu z_\nu] / (|\mathbf{z}|^3 |\mathbf{z} + \mathbf{x}|^3)$. As in the previous section, the variables $\mathbf{x}, \mathbf{y}, \mathbf{z}$ have been rescaled with respect to the original ones in order to extract the behavior in L_1 . Again, if $L_1, L_2 \gg \xi$ the analytical evaluation of $C(t, t')$ becomes possible, leading to

$$N_2 = -\frac{V L_2^{-1/2} L_1^{-1}}{(2\pi)^6} M^{3/2} 4K, \quad (19)$$

where K is the constant $\frac{1}{6} B(\frac{3}{2}, \frac{1}{2}) + \frac{1}{2} B(\frac{5}{2}, \frac{1}{2}) - B(\frac{7}{2}, \frac{1}{2}) + \frac{1}{3} B(\frac{9}{2}, \frac{1}{2}) = 19\pi/384 \approx 0.154$, and $B(a, b)$ is the Beta function. For large $L_1 \rightarrow \infty$, this diagram gives a negligible contribution with respect to N_1 .

The third diagram in Fig. 2 give the same as the second, except that L_1 and L_2 are interchanged: $N_3 = N_2|_{L_1 \leftrightarrow L_2}$.

8. The fourth Feynman diagram in Fig. 2 has no ultraviolet divergence. As before, it can be exactly evaluated

apart from the lattice integrations. However, the behavior of the related Feynman integral N_4 can be easily estimated in the following limits:

1. $L_1 \gg 1; L_1 \gg L_2$, where $N_4 \propto L_1^{-1}$,
2. $L_2 \gg 1; L_2 \gg L_1$ where $N_4 \propto L_2^{-1}$,
3. $L_1, L_2 \gg 1$, $L_2/L_1 = \text{finite}$, where $N_4 \propto L_1^{-3/2}$.

Moreover, if the lengths of the polymers are considerably larger than the persistence length, N_4 can be computed in a closed form:

$$N_4 \approx -\frac{128V}{\pi^5} \frac{M}{\pi^{3/2}} (L_1 L_2)^{-1/2} \times \int_0^1 ds \int_0^1 dt (1-s)(1-t)(st)^{1/2} \times [L_1 t(1-s) + L_2(1-t)s]^{-1/2}. \quad (20)$$

It is simple to check that this expression has exactly the above behaviors.

9. Collecting all contributions we obtain the result for the second topological moment $\langle m^2 \rangle = (N_1 + N_2 + N_3 + N_4)/Z$, with N_1, N_2, N_3, N_4, Z given by Eqs. (13), (16), (19), and (20). In all formulas, we have assumed that the volume V of the system is much larger than the size of the volume occupied by a single polymer, i.e., $V \gg L_1^3$.

To discuss the physical content of the above expression for $\langle m^2 \rangle$, we consider a number N_p of polymers $p_1 \dots p_{N_p}$ with lengths $l_1 \dots l_{N_p}$ in an uniform solution. We introduce the polymer concentration $\rho = \mathcal{M}/V$ as the average mass density of the polymers per unit volume, where \mathcal{M} is the total mass of the polymers $\mathcal{M} = \sum_{k=1}^{N_p} m_a l_k/a$ and m_a is the mass of a single monomer of length a . Thus l_k/a is the number of monomers in the polymer p_k . The polymer P_1 is singled out as anyone of the polymers p_k , say $p_{\bar{k}}$, of length $L_1 = l_{\bar{k}}$. The remaining ones are replaced by a long effective polymer P_2 of length $L_2 = \sum_{k \neq \bar{k}} l_k$. From the above relations we may also write

$$L_2 \approx \frac{aV\rho}{m_a}. \quad (21)$$

In this way, the length of the effective molecule P_2 is expressed in terms of physical parameters. Keeping only the leading terms for $V \gg 1$, we find for the average square number of intersections $\langle m^2 \rangle_{sol}$ formed by P_1 with the other polymers the approximate result

$$\langle m^2 \rangle_{sol} \approx \frac{N_1 + N_2}{Z}, \quad (22)$$

which, in turn, has the approximate form

$$\langle m^2 \rangle_{sol} = \frac{a\rho}{m_a} \left[\frac{\xi^{-1} L_1}{2\pi^{1/2} M^2} - \frac{2K L_1^{1/2}}{\pi^4 M^{3/2}} \right], \quad (23)$$

with K as defined after Eq. (19). This is the announced final result. Since the persistence length is of the same order of the monomer length a and $M \sim a^{-1}$, $\langle m^2 \rangle$ is positive for large L_1 as it should.

10. In conclusion, we have found an exact field theoretic formula for the second topological moment of two polymers. Only the final integrations over the spatial variables in the Feynman diagrams of Fig. 2 were done approximately. These were defined on a lattice related to the finite monomer size. Our Chern-Simons-based theory is free of the shortcomings of previous mean-field procedures. Our formula for $\langle m^2 \rangle$ has been applied to the realistic case of long flexible polymers in a solution. When the polymer lengths become large, the Feynman integrals in N_1, \dots, N_4 can be evaluated analytically. In this way we have been able to derive the result (23) for the average square number of intersections formed by a polymer P_1 with all the others. This calculation is *exact* in the long-polymer limit. The corrections to (23) are suppressed by further inverse square roots of the polymer lengths.

To leading order in L_1 , our result (23) agrees with that of [9], but our exact subleading correction goes beyond the approximation of [9]. Note that there is no direct comparison of our result with that of [6], since there the polymer P_2 was considered as a fixed obstacle causing a dependence on the choice of the configuration of P_2 .

Finally, let us emphasize the absence of infrared divergences in the topological field theory (4) in the limit of vanishing masses $m_1, m_2 = 0$. As a consequence, the second topological moment does not diverge in the limit of large L_1 if $\langle m^2 \rangle$ is calculated from (4) for polymers passing through two fixed points $\mathbf{x}_1, \mathbf{x}_2$. This indicates a much stronger reduction of the configurational fluctuations by topological constraints than one might have anticipated.

-
- [1] M.G. Brereton, S. Shah, *J. Phys. A: Math. Gen.* **13**, (1980), 2751.
 - [2] M. G. Brereton and T. A. Vilgis, *Jour. Phys. A: Math. Gen.* **28** (1995), 1149.
 - [3] M. Otto and T. A. Vilgis, *Phys. Rev. Lett.* **80** (1998), 881.
 - [4] J. D. Moroz and R. D. Kamien, *Nucl. Phys.* **B506** [FS] (1997), 695.
 - [5] F. Ferrari and I. Lazzizzera, *Nucl. Phys.* **B559** (3), (1999), 673.
 - [6] F. Tanaka, *Prog. Theor. Phys.* **68** (1), (1982), 148.
 - [7] H. Kleinert, *Path Integrals in Quantum Mechanics Statistics and Polymer Physics*, World Scientific, Singapore, 1995.
<http://www.physik.fu-berlin.de/~kleinert/re.html#b5>
 - [8] S. F. Edwards, *Proc. Phys. Soc.* **91** (1967), 51.
 - [9] M.G. Brereton, S. Shah, *J. Phys. A: Math. Gen.* **15**, (1982), 985.